Numerical Simulation of an Improved CZTS/WS$_2$ PV Cell by SCAPS 1-D

A.A.Md. Monzur-Ul-Akhir and Md Touhidul Imam

Abstract—CZTS solar cells are promising among the third-generation solar cell. Because of its earth abundant materials and less toxicity CZTS solar cell can perform a sustainable role as an absorber layer. The optimization of a buffer layer is still a challenge and efficiency are still low than other thin film solar cells. In this study, WS$_2$ buffer layer have been used to simulate the PV cell structure in SCAPS-1D simulation software. No research has been found where CZTS and WS$_2$ is used together. We have achieved a maximum efficiency of η = 18.90 % at 300 K working temperature and other factors i.e., Voc, Jsc and FF are also promising. The highest certified efficiency of CZTS solar cell is nearly 12%. The simulation profile can be a guideline for fabricating the improved PV cell.

Index Terms— Solar cell, CZTS, WS$_2$, SCAPS-1D, Buffer layer.

I. INTRODUCTION

THE renewable energy sources are proving to be more potential and convenient method of generating electrical power. Solar, wind, geothermal, wave energy are the examples of renewable energy sources. Among these energy sources solar energy is easy to use as it converts light into electrical energy. But the conversion efficiency is less than 30% [1]. Typically, solar cell is classified into three generations. Silicon wafer solar cells are the first-generation solar cell [2-3]. Amorphous Si, CIGS (Cu(lnGa)Se), CdTe are the second-generation solar cells. Third generation solar cells are perovskite, CZTS (Cu$_2$ZnSnS$_4$), etc. [4-6]. Si can be considered as most widely used absorber materials. Though it's low throughput and high cost, it has an efficiency of 26.7 ± 0.5 % [7]. Second generation CIGS and CdTe solar cell efficiency is achieved upto 23% and 21% respectively [8].

A.A.Md. Monzur-Ul-Akhir is with Green University of Bangladesh, Dhaka, Bangladesh. Email: monzur@eee.green.edu.bd.

Md Touhidul Imam is with Green University of Bangladesh, Dhaka, Bangladesh. E-mail: messut.imamsharif@gmail.com

But these two materials inherit high toxicity for cadmium and selenium. Other than that tellurium and indium are less available [9]. To overcome these problems researchers have been considering CZTS (Cu$_2$ZnSnS$_4$) as a good absorbing material for the past decade. Main objective of this study is to improve efficiency of CZTS solar cell aided with WS$_2$ additional layer. Focus was to improve the efficiency more than 12% [8]. In this paper we have studied CZTS/WS$_2$ based solar cell structure with the help of SCAPS-1D solar cell simulation and modeling software. We have observed the effect of variation in WS$_2$ layer thickness, CZTS layer thickness and temperature. We have also taken into consideration of the effect of shallow acceptor density of CZTS absorber material and shallow donor density of the WS$_2$ buffer layer. Based on the simulation an optimum design for CZTS/WS$_2$ structured solar cell is proposed. Generally, CdS is used as a buffer layer of a CZTS solar cell.

II. RELATED WORKS

CZTS (Copper Zinc Tin Sulfide) is a compound semiconductor. This has non-toxic earth abundant materials. It exhibits photovoltaic properties like CIGS and CdTe. It has an absorption coefficient above 10^4 cm^{-1} and direct band gap ranges from 1.4 to 1.6 eV [10-11]. For the buffer layer of CZTS solar cell many researchers are using CdS, ZnS and CdZnS [12]. Cadmium sulfide. CZTS (Copper Zinc Tin Sulfide) is a compound semiconductor. This has non-toxic earth abundant materials. It exhibits photovoltaic properties like CIGS and CdTe. It has an absorption coefficient above 10^4 cm^{-1} and direct band gap ranges from 1.4 to 1.6 eV [10-11]. For the buffer layer of CZTS solar cell many researchers are using CdS, ZnS and CdZnS [12]. Cadmium sulfide (CdS) proved to be most potential buffer layer for CZTS absorber layer for its suitable bandgap and interface enhancing properties. But CdS has high toxic component and can affect the environment with its wastage [13]. Besides maximum efficiency for CZTS solar cell has been reported less than 12% [14]. Lately, the TMDCs (transition metal di-chalcogenides), mainly MoS$_2$ (Molybdenum disulfide) and WS$_2$ (Tungsten disulfide) postured specific concerns for the solar cell material researchers because of their unique optoelectronic properties as
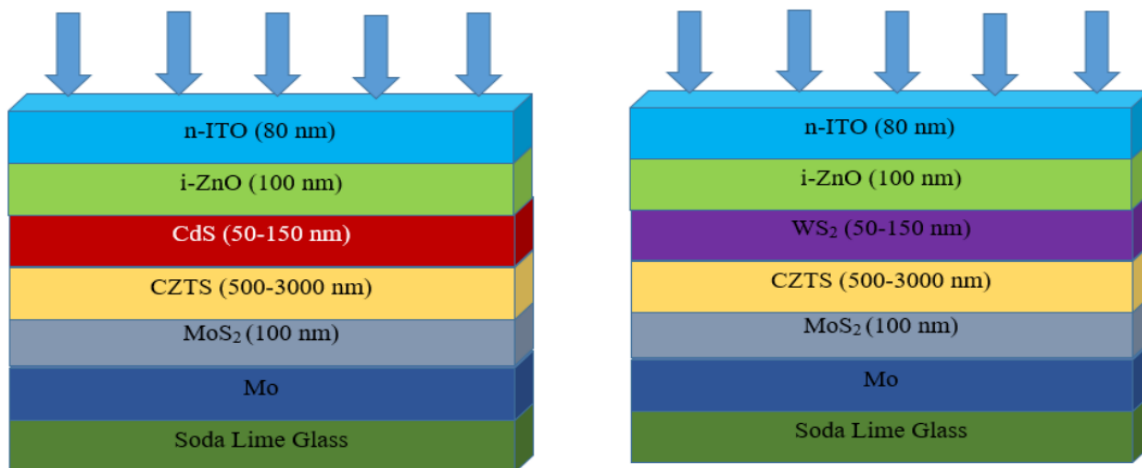
Fig. 1. Device structure of CZTS/WS2 solar cell (a) conventional structure (b) Proposed structure.

well as electrochemical properties of these materials [15]. Between these two materials WS$_2$ exhibits n-type semiconducting properties with better conductivity of $10^{-3}\Omega^{-1}cm^{-1}$[16]. Besides, WS$_2$ is an earth abundant material and has a bigger atom size [17]. Counter electrode in a dye-sensitized solar cell, ammonia gas sensors, thermoelectric material and super capacitors are the example of use of WS$_2$ material [18-21]. We have found research paper corresponding with CIGS/WS$_2$ and CdTe/WS$_2$ solar cell [22-23]. But no research found with CZTS/WS$_2$ structured solar cell. WS$_2$ can adopt graphite-like structured or can form quantum dots Nanoparticles. The band gap of WS$_2$ is 1.35 eV to 2.1 eV and the absorption of light region expands to 910 nm [24].

III. STRUCTURE AND PARAMETERS

A. Device Structure

The conventional Cu$_2$ZnSnS$_4$ based solar cell is structured on soda lime glass substrate where Mo is grown through thermal evaporation [25]. On the top of Mo material, CZTS materials are deposited where a thin layer of MoS$_2$ will produce [26]. CZTS layer works as a p-type absorber layer. Most of the incident photons are absorbed by this layer to generate electron hole pair [27]. Next to the absorber layer is buffer layer where n-CdS is used in the conventional thin film solar cells. Then n-ZnO (Zinc Oxide) is used for the window layer and finally, ITO (Indium doped Tin Oxide) or FTO (means what?) as a front contact layer of this categorized solar cells [28]. Buffer layer is used such a way that it could align with the band energy of the absorber layer [29]. Largely, the thickness of the absorber layer is 1000 nm to 3000 nm and the buffer layer thickness is very small only 50 nm to 150 nm. Consequently, the thickness of the window layer is between 60 nm to 100 nm. Primary purpose of the window layer is to maximize the incident photons to the CZTS and CdS layer [30]. ITO/FTO is used as a transparent conducting layer which increases the carrier mobility by obtaining a lower sheet resistance [31]. Fig. 1(a) shows the conventional CZTS based solar cell structure. In our study, we have used WS$_2$ as a buffer layer to observe the solar cell performance via software simulation. Fig.1(b) show the device structure of the solar cell of this study. Hereafter, we have proposed a solar cell structure as Mo/CZTS/WS$_2$/ZnO/ITO.

TABLE 1. PHYSICAL PARAMETERS OF THE MATERIALS

Parameters	MoS$_2$[12]	CZTS [12]	WS$_2$[23]	i-ZnO[12]	n-ITO [12]
Thickness (nm)	100	500-3000	50-150	100	80
Band gap (eV)	1.7	1.5	2.1	3.3	3.6
Electron affinity (eV)	4.2	4.5	4.1	4.6	4.1
Dielectric permittivity	13.6	10	13.6	9	10
CB effective density of states (cm^{-3})	2.2×10^{18}	2.2×10^{18}	2×10^{18}	2.2×10^{18}	2.2×10^{18}
VB effective density of states (cm^{-3})	1.8×10^{19}	1.8×10^{19}	2×10^{18}	1.8×10^{19}	1.8×10^{19}
Electron thermal velocity (cm s^{-1})	1×10^{7}	1×10^{7}	1×10^{7}	1×10^{7}	1×10^{7}
Hole thermal velocity (cm^{-1})	1×10^{7}	1×10^{7}	1×10^{7}	1×10^{7}	1×10^{7}
Electron mobility (cm^2/V$_s$)	100	100	100	100	50
Hole mobility (cm^2/V$_s$)	25	25	25	25	75
Shallow uniform donor density (cm^{-3})	0	1×10^{1}	1×10^{15}	1×10^{18}	1×10^{19}
Shallow uniform acceptor density (cm^{-3})	1×10^{16}	2×10^{14}	0	0	0
Defect type	-	Donor	Acceptor	-	-
Defect density (cm^{-3})	-	1×10^{15}	1×10^{13}	-	-
Absorption coefficient(cm^{-1})		10^{4}	10^{4}	Scaps value	Scaps Value

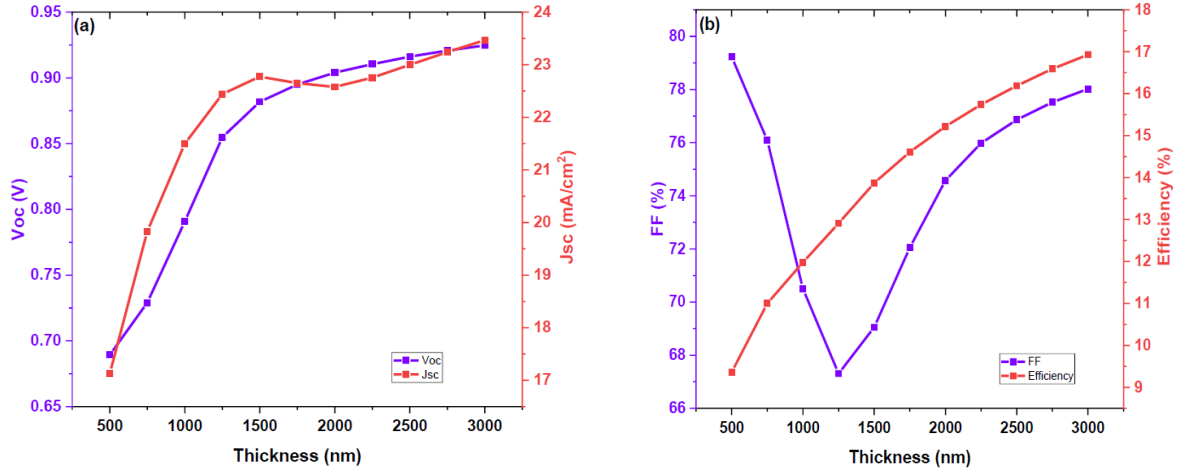## B. Validation of Structure

Fig.2 Absorber layer thickness variation (a) Voc, Jsc; (b) FF, Efficiency.

PV cell performance can be analyzed by J-V characteristic curve. We will validate the proposed structure by this J-V characteristic curve. Other than that, we will also make discussion over quantum efficiency. The fundamental equations that run the solar cell characteristics like Voc, Jsc, FF and efficiency can be expressed as

$$I = I_{ph} - I_o e^{\left(\frac{qV}{nk_BT}\right)} \ldots\ldots\ldots (1)$$

$$I_{sc} = I_o \left[e^{\left(\frac{qV_{oc}}{nk_BT}\right)} - 1 \right] \ldots\ldots\ldots(2)$$

$$V_{oc} = \frac{nk_BT}{q} \ln(\frac{I_{ph}}{I_o}) \ldots\ldots\ldots (3)$$

Where, I_{ph} is photo-generated current, I_o is reverse saturation current, n & k_B is the ideality factor and Boltzmann constant respectively. Using voltage current density curve, we can determine the I_{sc} (short-circuit current) at V=0 and V_{oc} (open circuit voltage) at I=0. We can calculate these from equation (2) and (3).

C. Simulation Software & Material Parameter

In this research simulation software named SCAPS-1D (Solar Cell Capacitance Simulator) is used to do the simulation. SCAPS-1D is one-dimensional solar cell simulation software, is developed by the dept. of EIS, University of Gent, Belgium. Material properties like band gap, electron and hole mobility, dielectric permittivity, electron affinity and other properties for different layer can be attuned in the layer properties panel [29]. SCAPS functionality depends on three differential equations. One of the equations is known as Poisson's equation and other two are continuity equation for electron and hole. The equations are respectively

$$\frac{\partial}{\partial x}\left(\varepsilon(x)\frac{\partial\Psi}{\partial x}\right) = -\frac{q}{\varepsilon_o}\left[-n + p + N_D - N_A + \frac{1}{q}\rho_{def}(n,p)\right] \ldots\ldots\ldots\ldots\ldots\ldots\ldots\ldots\ldots\ldots(4)$$

$$\frac{1}{q}\frac{\partial J_n}{\partial x} + G - R_n(n,p) = \frac{\partial n}{\partial t} \ldots\ldots\ldots\ldots\ldots (5)$$

$$-\frac{1}{q}\frac{\partial J_p}{\partial x} + G - R_p(n,p) = \frac{\partial p}{\partial t} \ldots\ldots\ldots\ldots (6)$$

Where, Ψ & ϵ are electrostatic potential and dielectric constant and ϵ_o is the permittivity in vacuum., n, p are carrier concentration of electron and hole respectively. N_D and N_A are donor and acceptor density and ρ_{def} is the defect density. R_n, R_p are combination rate of electron and hole, G is the generation rate and J_p & J_n are the current density of hole and electron.

The light illumination was through the n-ITO layer side with 1.5 global air mass spectrums with 1000W/m² at 298 K. We have included two types of single layer defects in CZTS for the simulation. Neutral type defect and single donor defect was considered for the CZTS material to perform the simulation and get more practical result. The simulation is performed in several steps. At first, the absorber layer thickness (500 nm - 3000 nm) was varied and then the buffer layer thickness (50 nm -150 nm). Next, the doping concentration was taken into consideration for both absorber and buffer layer. The shallow acceptor density of the CZTS material and shallow donor density (5.5×10^{12} to 5.5×10^{18} cm⁻³) of the WS2 material (1×10^{15} to 1×10^{20} cm⁻³) was varied during the simulation. All other simulation results like QE (Quantum Efficiency), generation-recombination, band diagram of the proposed structure and J-V characteristics graph have been observed and analyzed. All the physical
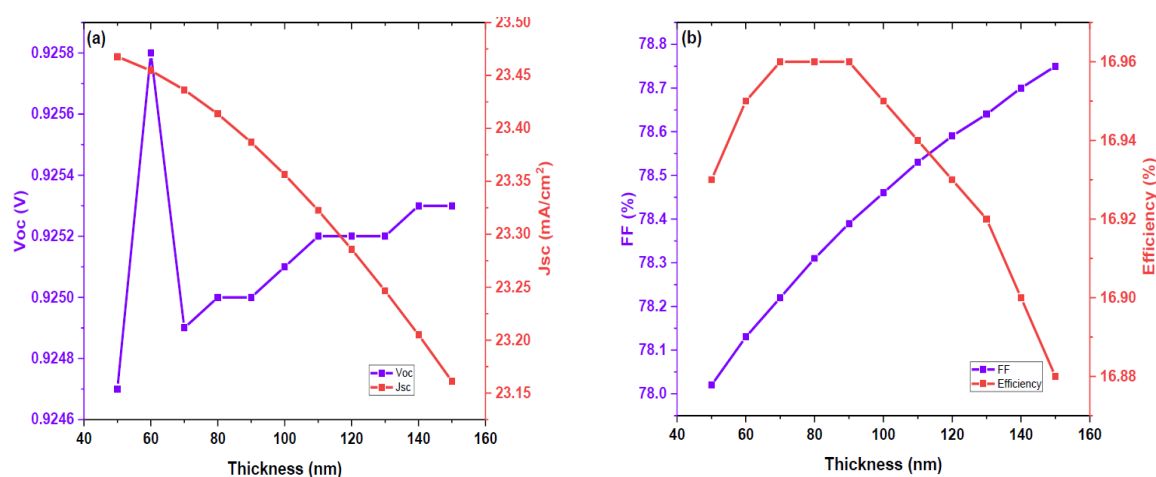
Fig.3. Buffer layer thickness variation (a)Voc, Jsc; (b) FF, Efficiency

parameters which have been used in this study have been taken from several research papers, experimental study [12,23]. All the physical properties are summarized in Table 1 [12, 17, 32-35]. The physical parameters of the materials which are used in this study are assembled in Table. 1.

IV. RESULT & DISCUSSION

The results of the simulation are discussed in three steps. At first, we have discussed about the buffer layer thickness. In this stage, we have kept absorber layer constant. After that we have kept buffer layer fixed and observed the absorber layer thickness variation. Then absorber layer thickness and buffer layer thickness have been kept constant and we varied the working temperature to find the optimum output. In this way we have systematically established the optimized structure.

A. Absorber Layer Thickness

To observe the absorber layer thickness variation, the buffer layer thickness was kept at 50 nm. Then the CZTS layer thickness has been varied from 500 nm to 3000 nm and the electrical parameters data have been collected to analyze the variation. Fig. 2 shows the simulation data collected from the software through graphical presentation. Fig. 2(a) shows the Voc and Jsc change over thickness variation of absorber layer. As the thickness increases from 500 nm to 3000 nm both Voc and Jsc increases. Voc increases rapidly from 0.6894 V to 0.08549 V for the thickness change from 500 nm to 1250 nm. After that the rate of increase of the Voc starts to decrease. At 3000 nm it shows 0.9247V of open circuit voltage. Short circuit current density (Jsc) also increases like Voc. From 500 nm to 1500 nm Jsc increase almost linearly but after that the Jsc decreases for increasing of absorber layer thickness. Data show that Jsc increases from 17.1290

mA/cm2 to 22.7739 mA/cm2 as the thickness changes from 500 nm to 1500 nm. This happens because as the thickness of the absorber layer increases more photons are absorbed by the layer thus creates more photogeneration. For that as the thickness increases open circuit voltage and short circuit current increases. From eqn. (1) we can see that if the I_{ph} increases the current also increases. And if the I_{ph} increase the V_{oc} also increases as it was shown in eqn. (3). From 1500 nm thickness the short circuit current starts to fall (22.5789 mA/cm2) and after 2000 nm it starts to increase again. At 3000 nm the value of Jsc becomes 23.47 mA/cm2. Fig. 2(b) shows the fill factor and efficiency graph for thickness the thickness increases open circuit voltage and short circuit current increases. From eqn. (1) we can see that if the I_{ph} increases the current also increases. And if the I_{ph} increase the V_{oc} also increases as it was shown in eqn. (3). From 1500 nm thickness the short circuit current starts to fall (22.5789 mA/cm2) and after 2000 nm it starts to increase again. At 3000 nm the value of Jsc becomes 23.47 mA/cm2. Fig. 2(b) shows the fill factor and efficiency graph for thickness 3000 nm and varied the buffer layer thickness and observe the solar cell parameters.

B. Buffer Layer Thickness Variation

We have investigated the data from the simulation of the stricture shown in fig.1. We have kept the CZTS absorber layer at 3000 nm thick. The buffer layer thickness was varied from 50 nm to 150 nm at 10 nm difference. A single acceptor type defect was taken into consideration with a defect density of 1×10^{14} cm^{-3} in the WS$_2$ buffer layer. Fig. 3. Shows the data we have collected from the simulation of different parameters like open-circuit voltage (Voc), short-circuit current density (Jsc), fill-factor (FF) and efficiency (η) by varying the thickness of the buffer layer. Voc increase sharply at 60 nm and after that the Voc decreases. After
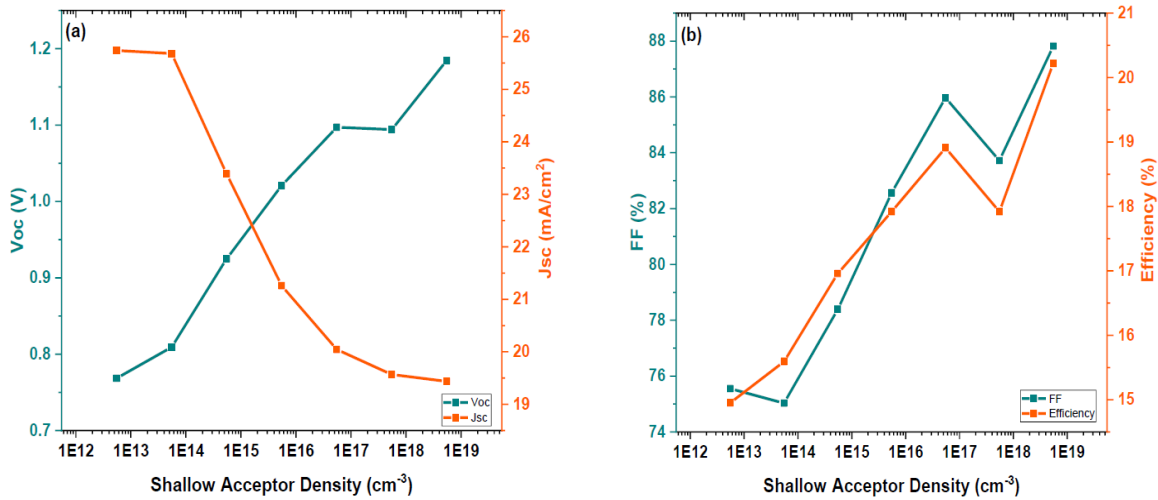
Fig.4. Shallow acceptor density variation of absorber layer (a) V0c, Jsc; (b) FF, Efficiency

70 nm the Voc starts to increase and at 150 nm the Voc becomes 0.9253 V. Fig. 3(a) shows the Voc variation graph of buffer layer thickness variation. But the scenario for the Jsc is quite different. The short circuit density decreases from 23.46 mA/cm² to 23.16 mA/cm². The change in Jsc is very low. So, it can be said that the variation of thickness of the buffer layer didn't affect the Jsc very much. The fill factor increases if the thickness of the buffer layer is increased but the rate of increment is very low. It remains between 78.0 % and 78.8%. But the efficiency of the solar cell depends on the thickness of the buffer layer. In general, the thickness of the buffer layer is50 nm if we use CdS as a buffer layer. But in this research, we have observed that efficiency starts to increase at first but after 70 nm to 90 nm it remains constant. But if we increase the thickness of the buffer layer more, the efficiency starts to decrease. We have taken our optimum buffer layer thickness to 90 nm because at this thickness the efficiency was at pick and the fill factor was also reasonable.

C.   Shallow Acceptor Density Variation

As it is known that doping creates a depletion layer in the p-n junction photovoltaic solar cell. So, the variation of doping concentration creates different depletion layer width which creates different electric field for photons generated carrier for flowing. In this part we have kept the thickness of the CZTS layer at 3000 nm and the thickness of the buffer layer at 90 nm. But we have varied the acceptor density of the CZTS layer because the CZTS layer is working as a p-type material where the hole of the material is ready to create recombination with electron. The acceptor density varied from 5.5×10^{12} cm⁻³ to 5.5×10^{18} cm⁻³. The effect of the variation of acceptor density is shown in Fig. 4. Voc increases almost linearly from 5.5×10^{12} cm⁻³ to 5.5×10^{16} cm⁻³ of acceptor density. This time,

it increases from 0.75 V to 1.06 V and after that it remains constant for a further increment of the density. But after 5.5×10^{17} cm⁻³, it starts to increase again. Jsc show different scenario for acceptor density variation. Short circuit current density decreases from 25.73 mA/cm2 to 19.43 mA/cm² as the acceptor density of the absorber layer increases. If the acceptor density of the CZTS layer increased, the simulation data shows that, fill factor and efficiency both increase for increasing density. The graph shows that the efficiency and fill factor both increases linearly at the density variation from 5.5×10^{12} cm⁻³ to 5.5×10^{16} cm-3 after that it decreases a bit and again starts to increase. At 5.5×10^{16} cm⁻³ FF becomes 86% and the efficiency becomes 18.90%. Fig. 4(b) shows the graph of fill factor and efficiency. We have selected our shallow acceptor density 5.5×10^{16} cm⁻³ because to have more practical oriented data.

D.   Shallow Donor Density Variation

We have also analyzed the shallow donor density variation of the WS₂ buffer layer to optimize our device structure. WS₂ is the high doped n-type layer. The practical density can be achieved up to 1.0×10^{20} cm⁻³. The donor density was varied from 1.0×10^{15} cm⁻³ to 1.0×10^{20} cm⁻³. At this time the shallow acceptor density of the absorber layer was kept at 5.5×10^{16} cm⁻³. Fig. 5 shows the graph of various electrical parameter of the solar cell device. Open circuit voltage (Voc) of the device increases from 0.98V to 1.09V because of increasing the donor density of the layer up to 1.0×10^{18} cm⁻³. After that it remains at this level upto the donor density of 1.0×10^{20} cm⁻³. Jsc also increase from 18.50 mA/cm² to 20.04 mA/cm² at the layer donor density increase from 1.0×10^{15} cm⁻³ to 1.0×10^{18} cm⁻³. After that it starts to decrease. Fig. 5(a) shows the data graph of Voc and Jsc. same scenario happened for the fill factor and efficiency of the solar cell device.
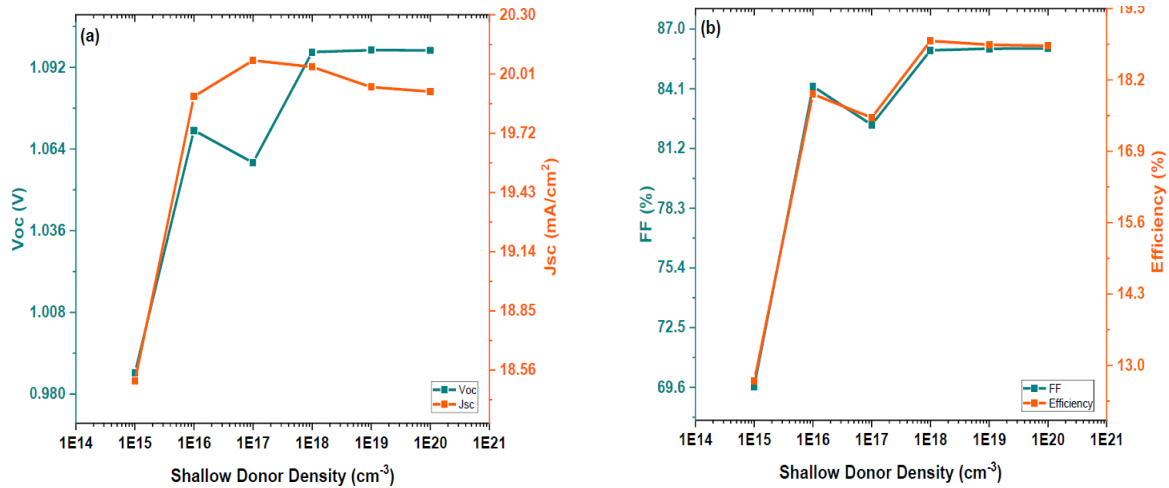
Fig.5. Shallow donor density variation of buffer layer (a) Voc, Jsc; (b) FF, Efficiency

Both increases sharply for increasing the value of shallow donor density. But after 1.0×10^{18} cm^{-3} FF and efficiency remain nearly constant. Efficiency starts to decrease after 1.0×10^{18} cm^{-3}. After this level we have selected our shallow donor density of the device at 1.0×10^{18} cm^{-3}.

V. PROPOSED PARAMETER FOR STRUCTURE

After analyzing the data collected from the simulation, we are proposing a thin film of CZTS/WS$_2$ based solar cell parameter for optimum efficiency and FF. We have chosen buffer layer thickness of 90 nm and absorber layer thickness at 3000 nm, where Vmpp is 0.9 V and Jmpp is 19.02 mA/cm^2. The fill factor and efficiency are also promising in this thickness of the buffer layer. Other layers like, intrinsic ZnO (Zinc Oxide) and n-ITO (Indium doped Tin Oxide) is taken

100 nm and 80 nm respectively. Table 2 shows the optimum thickness for all layers and Table 3 shows the simulated measured values of Voc, Jsc, FF, efficiency, Vmpp and Jmpp at 300K working temperature. We have also observed the quantum efficiency graph of our device which is shown in Fig. 6. The quantum efficiency is highest between 400nm to 700nm after that the quantum efficiency starts to decrease. This happens because quantum efficiency depends on surface recombination. Probability of collecting photons also make an effect on solar cell quantum efficiency.

TABLE 2. OPTIMUM LAYER THICKNESS OF THE DEVICE

Material	MoS$_2$	CZTS	WS$_2$	i-ZnO	n-ITO
Thickness (nm)	100	3000	90	100	80

TABLE 3. MEASURED PARAMETER AT OPTIMUM THICKNESS

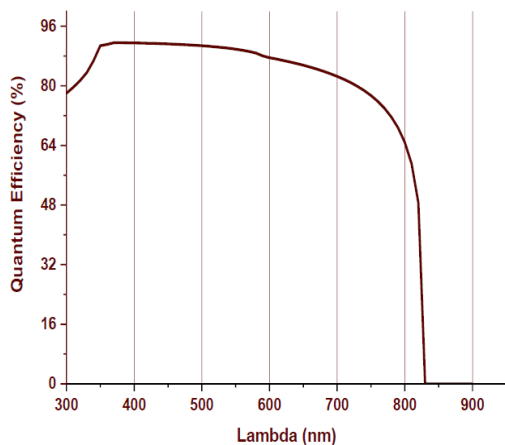| Voc (v)	Jsc (mA/cm^2)	FF (%)	η (%)	Vmpp (v)	Jmpp (mA/cm^2)
1.09	20.04	85.96	18.90	0.99	19.03

Fig.6. Quantum efficiency of the device.

VI. FUTURE SCOPE

. WS$_2$ semiconductor material can be used with other solar cells like CIGS, a-Si, perovskite etc. From this simulation's result we find that the efficiency increases with the working temperature. Monzur-Ul-Akhir at el.proposed that high temperature affects the conversion ratio and in the Middle East countries despite of having high irradiance the conversion ratio is lower than other low-irradiance countries [36]. In high ambient temperature countries this type of solar cell can play a vital role. One work has been done on suitable surrounding for solar cell conversion rate, we

have seen that low temperature (4°C -9°C) improves the conversion rate [37].

VII. CONCLUSION

In this study numerical simulation of CZTS solar cell with WS₂ buffer layer was carried out by SCAPS-1D software to study the solar cell performance. Solar cell parameters were observed by varying the absorber layer thickness, buffer layer thickness, shallow acceptor density, shallow donor density. The J-V curve confirms the proposed structure and exhibit 18.90 % efficiency. High open circuit voltage dominates the J-V curve. As we can observe from the simulated data substituting CdS by WS₂ as a buffer layer improves the efficiency about 6%. Increasing the carrier concentration, the performance parameter can be improved. We have also showed the temperature variation of our proposed structure and this case solar cell performance decreases for increasing working temperature. Nevertheless, it has been observed from our study that introducing WS₂ as a buffer layer of a CZTS solar cell improves the cell performance.

REFERENCES

[1] Fatemi Shariat Panahi, S. R., Abbasi, A., Ghods, V., &Amirahmadi, M. (2020). Analysis and improvement of CIGS solar cell efficiency using multiple absorber substances simultaneously. Journal of Materials Science: Materials in Electronics, 31(14), 11527–11537.

[2] Green, M. A. (2000). Photovoltaics: technology overview. Energy policy, 28(14), 989-998.

[3] Liou, H. M. (2010). Overview of the photovoltaic technology status and perspective in Taiwan. Renewable and Sustainable Energy Reviews, 14(4), 1202-1215.

[4] Green, M. A. (2002). Third generation photovoltaics: solar cells forn2020 and beyond. Physica E: Low-dimensional Systems and Nanostructures, 14(1-2), 65-70.

[5] Bagher, A. M., Vahid, M. M. A., & Mohsen, M. (2015). Types of solarcells and application. American Journal of optics and Photonics, 3(5), 94-113

[6] Rao, S., Morankar, A., Verma, H., &Goswami, P. (2016). Emergingphotovoltaics: organic, copper zinc tin sulphide, and perovskite-based solar cells. J. Appl. Chem, 2016, 3971579.

[7] Green, M. A., Dunlop, E. D., Hohl-Ebinger, J., Yoshita, M., Kopidakis, N., &Hao, X. (2020). Solar cell efficiency tables (version56). Progress in Photovoltaics: Research and Applications, 28(NREL/JA-5900-77544).

[8] Green, M. A., Emery, K., Hishikawa, Y., Warta, W., Dunlop, E. D.,Levi, D. H., & Ho-Baillie, A. W. (2017). Solar cell efficiency tables (version 49). Progress in photovoltaics: research and applications, 25(1), 3-13.

[9] Yeh, M. Y., Lei, P. H., Lin, S. H., & Yang, C. D. (2016). Copper-zinctin-sulfur thin film using spin-coating technology. Materials, 9(7), 526.

[10] Katagiri, H., Saitoh, K., Washio, T., Shinohara, H., Kurumadani, T., &Miyajima, S. (2001). Development of thin film solar cell based on Cu2ZnSnS4 thin films. Solar Energy Materials and Solar Cells, 65(1-4), 141-148.

[11] Zakaria, Z., Chelvanathan, P., Rashid, M. J., Akhtaruzzaman, M.Alam, M. M., Al-Othman, Z. A. ...& Amin, N. (2015). Effects of sulfurization temperature on Cu2ZnSnS4 thin film deposited by single source thermal evaporation method. Japanese Journal of Applied Physics, 54(8S1), 08KC18.

[12] Jhuma, F. A., Shaily, M. Z., & Rashid, M. J. (2019). Towards highefficiency CZTS solar cell through buffer layer optimization. Materialsfor Renewable and Sustainable Energy, 8(1), 1-7.

[13] Li, X., Yang, X., Yuwen, L., Yang, W., Weng, L., Teng, Z., &Wang,(2016). Evaluation of toxic effects of CdTe quantum dots on the reproductive system in adult male mice. Biomaterials, 96, 24-32.

[14] Yan, C., Huang, J., Sun, K., Johnston, S., Zhang, Y., Sun, H. ...&Hao,(2018). Cu 2 ZnSnS 4 solar cells with over 10% power conversion efficiency enabled by hetero-junction heat treatment. Nature Energy, 3(9), 764-772.

[15] Dasgupta, U., Chatterjee, S., & Pal, A. J. (2017). Thin-film formation of 2D MoS2 and its application as a hole-transport layer in planar perovskite solar cells. Solar Energy Materials and Solar Cells, 172, 353-360.

[16] Hankare, P. P., Manikshete, A. H., Sathe, D. J., Chate, P. A., Patil, A. A., &Garadkar, K. M. (2009). WS2 thin films: Opto-electronic characterization. Journal of alloys and compounds, 479(1-2), 657-660.

[17] Gusakova, J., Wang, X., Shiau, L. L., Krivosheeva, A., Shaposhnikov, V., Borisenko, V. ...&Tay, B. K. (2017). Electronic properties of bulk and monolayer TMDs: theoretical study within DFT framework (GVJ-2e method). physica status solidi (a), 214(12), 1700218.

[18] Hussain, S., Patil, S. A., Memon, A. A., Vikraman, D., Abbas, H. G., Jeong, S. H., ... & Jung, J. (2018). Development of a WS2/MoTe2 hetero-structure as a counter electrode for the improved performance in dye-sensitized solar cells. Inorganic Chemistry Frontiers, 5(12), 3178-3183.

[19] Li, X., Li, X., Li, Z., Wang, J., & Zhang, J. (2017). WS2 Nanoflakes based selective ammonia sensors at room temperature. Sensors andActuators B: Chemical, 240, 273-277.

[20] Liang, A., Li, D., Zhou, W., Wu, Y., Ye, G., Wu, J. ...& Du, Y. (2018). Robust flexible WS2/PEDOT: PSS film for use in high-performance miniature supercapacitors. JournalofElectroanalyticalChemistry, 824, 136-146.

[21] Kim, J. H., Yu, S., Lee, S. W., Lee, S. Y., Kim, K. S., Kim, Y. A., & Yang, C. M. (2020). Enhanced Thermoelectric Properties of WS2/Single-Walled Carbon Nanohorn Nanocomposites. Crystals, 10(2), 140.

[22] Rafiq, M. K. S. B., Amin, N., Alharbi, H. F., Luqman, M., Ayob, A., Alharthi, Y. S. ...&Akhtaruzzaman, (2020). WS 2: a new window layer material for solar cell application. Scientific reports, 10(1), 1-11.

[23] Sobayel, K., Shahinuzzaman, M., Amin, N., Karim, M. R., Dar, M. A., Gul, R. ...&Akhtaruzzaman, M. (2020). Efficiency enhancement of CIGS solar cell by WS2 as window layer through numerical modelling tool. Solar Energy, 207, 479-485.

[24] Sang, Y., Zhao, Z., Zhao, M., Hao, P., Leng, Y., & Liu, H. (2015).b From UV to near-infrared, WS2 nanosheet: a novel photocatalyst for full solar light spectrum photodegradation. Advanced materials, 27(2), 363-369.

[25] Shin, B., Gunawan, O., Zhu, Y., Bojarczuk, N. A., Chey, S. J., &Guha, S. (2013). Thin film solar cell with 8.4% power conversion efficiency using an earth-abundant Cu2ZnSnS4 absorber. Progress in Photovoltaics: Research and Applications, 21(1), 72-76.

[26] Yang, K. J., Sim, J. H., Jeon, B., Son, D. H., Kim, D. H., Sung, S. J., ... & Kang, J. K. (2015). Effects of Na and MoS2 on Cu2ZnSnS4 thin-film solar cell. Progress in Photovoltaic: Research and Applications, 23(7), 862-873.

[27] Jhuma, F. A., & Rashid, M. J. (2020). Simulation study to find suitable dopants of CdS buffer layer for CZTS solar cell. Journal of Theoretical and Applied Physics, 14(1), 75-84.

[28] Rana, M. S., Islam, M. M., &Julkarnain, M. (2021). Enhancement in efficiency of CZTS solar cell by using CZTSe BSF layer. Solar Energy, 226, 272-287.

[29] Inoue, Y., Hála, M., Steigert, A., Klenk, R., &Siebentritt, S. (2015, June). Optimization of buffer layer/i-layer band

alignment. In 2015 IEEE 42nd Photovoltaic Specialist Conference (PVSC) (pp. 1-5). IEEE.

[30] Kartopu, G., Clayton, A. J., Brooks, W. S., Hodgson, S. D., Barrioz, V., Maertens, A., ...& Irvine, S. J. (2014). Effect of window layer composition in Cd1− xZnxS/CdTe solar cells. Progress in Photovoltaics: Research and Applications, 22(1), 18-23.

[31] Hossain, S., Amin, N., Martin, M. A., Aliyu, M. M., Razykov, T., &Sopian, K. (2011). A NUMERICAL STUDY ON THE PROSPECTS OF HIGH EFFICIENCY ULTRA THIN Zn x Cd 1-x S/CdTe Solar Cell. Chalcogenide Letters, 8(4).

[32] Lin, P., Lin, L., Yu, J., Cheng, S., Lu, P., &Zheng, Q. (2014). Numerical simulation of Cu2ZnSnS4 based solar cells with In2S3 buffer layers by SCAPS-1D. Journal of Applied Science andEngineering, 17(4), 383-390.

[33] Mebarkia, C., Dib, D., Zerfaoui, H., &Belghit, R. (2016). Energyefficiency of a photovoltaic cell based thin films CZTS by SCAPS. Journal of Fundamental and Applied Sciences, 8(2), 363-371.

[34] Djinkwi Wanda, M., Ouédraogo, S., Tchoffo, F., Zougmoré, F., &Ndjaka, J. M. B. (2016). Numerical investigations and analysis of Cu2ZnSnS4 based solar cells by SCAPS-1D. International Journal ofPhotoenergy, 2016.

[35] Coutal, C., Azema, A., &Roustan, J. C. (1996). Fabrication and characterization of ITO thin films deposited by excimer laser evaporation. Thin Solid Films, 288(1-2), 248-253

[36] T. Imam & A. A. Md. Monzur-Ul-Akhir (2021). Analysis of solar photovoltaic performance in different global regions. Journal of Emerging Trends in Electrical Engineering. Volume 3 Issue 1. http://doi.org/10.5281/zenodo.4767172

Md Touhidul Imam was born in Faridpur, in 1990. He received the B.Sc. in Electrical & Electronic Engineering from the Green University of Bangladesh, in 2021. Currently he is studying MSc in Renewable Electricity Production in Uppsala University, Sweden. His research interests include hybrid renewable system, wind and wave power, advanced solar materials, and hydroelectric power.

A. A. Md. Monzur-Ul-Akhir was born in Dhaka. He is currently acting as an Assistant Professor in Electrical and Electronic Engineering Department, Green University of Bangladesh. He is also acting as an Associate Editor of the Green University of Bangladesh Journal of Science and Engineering (GUBJSE). He is an ex-Notredamian. He completed his Bachelors and Masters in EEE from the University of Dhaka. He also completed his MBA in Finance from the Institute of Business Administration (IBA) from the University of Dhaka in 2012. He got the prestigious merit scholarship from the Japanese Government-Monbukagakusho (Monbusho/MEXT) in 2014 to pursue his PhD in Nano and Functional Material Sciences from the University of Toyama. After his Ph.D. degree in 2018 he was then awarded with the "Marubun Research Promotion Foundation Grant 2018" to complete his Postdoctoral research from 2018-2019 at the University of Toyama. His research interest includes Group III-V Compound Semiconductors,Thin-film growth, Spintronics, Solar cell, Solar Materials, Nano-technology, Cryptography, Robotics, Electronic devices, Business studies, etc. He has worked for different Private Universities in Bangladesh from 2009-2019. He has achieved the professional certificate of Diplomaed Associate of The Institute of Bankers, Bangladesh (DAIBB). He attended the international conference ICIEV 2019,Washington, Spokane, USA, and his submitted paper won the best paper award. He has several Journal and Conference publications. He is currently appointed as the Moderator of "Green Theatre" -the theatre club of the Green University of Bangladesh.